

Dynamic Walking on Stepping Stones with Gait Library and Control Barrier Functions

Quan Nguyen¹, Xingye Da², J. W. Grizzle³, Koushil Sreenath¹

¹Dept. of Mechanical Engineering, Carnegie Mellon University, Pittsburgh, PA 15213

²Dept. of Mechanical Engineering, University of Michigan, Ann Arbor, MI 48109

³Dept. of Electrical Engineering and Computer Science, University of Michigan, Ann Arbor, MI 48109

Abstract. Dynamical bipedal walking subject to precise footstep placements is crucial for navigating real world terrain with discrete footholds such as stepping stones, especially as the spacing between the stone locations significantly vary with each step. Here, we present a novel methodology that combines a gait library approach along with control Barrier functions to enforce strict constraints on footstep placement. We numerically validate our proposed method on a planar dynamical walking model of MARLO, an underactuated bipedal robot. We show successful single-step transitions from a periodic walking gait with a step length of 10 (cm) to a stepping stone with a 100 (cm) separation (10x step length change), while simultaneously enforcing motor torque saturation and ground contact force constraints. The efficacy of our method is further demonstrated through dynamic walking over a randomly generated stepping stones requiring single-step step length changes in the range of [10:100] (cm) with a foot placement precision of 2 (cm).

1 Introduction

An important advantage of robotic systems employing legged locomotion is the ability to traverse terrain with discrete footholds, such as “stepping stones.” Current approaches to handling this form of terrain primarily rely on simplistic methods, both at the level of models of bipedal robots (e.g., linear inverted pendulum) and control (e.g., ZMP) to achieve the desired foot placements. The overarching goal of this work is to create a formal framework that will enable bipedal humanoid robots to achieve dynamic and rapid locomotion over a randomly placed, widely varying, set of stepping stones.

Footstep placement control for fully actuated legged robots initially relied on quasi-static walking and resulted in slow walking speeds [13],[14],[5]. Impressive results in footstep planning and placements in obstacle filled environments with vision-based sensing have been carried out in [15],[4]. The DARPA Robotics Challenge inspired several new methods, some based on mixed-integer quadratic

programs [7]. However, as mentioned in [8, Chap. 4], mixed-integer-based footstep planning does not offer dynamic feasibility even on a simplified model. These methods therefore are not applicable for dynamic walking with faster walking gaits. The approach developed in [22] allows aperiodic gaits with varying step lengths designed on a complete dynamical model, but requires the *a priori* design of controllers that realize precise transitions between each pair of elements of the gait library, resulting in exponential (factorial) growth in the number of pre-designed controllers.

Instead of relying on kinematics of quasi-static motion planning of simplified dynamical models, such as a linear inverted pendulum with massless legs [9],[20], this paper presents a novel control strategy based on the full nonlinear hybrid dynamic model of the robot and its environment that can achieve precise foot placement with formal stability and guarantees on physical constraints. We do this by combining a pre-computed library of walking gaits [6] with control-barrier-function-based quadratic programs (CBF-QPs) for enforcing stepping stone constraints [17,2]. The gait library is populated with a small number of feedback controllers that achieve asymptotically stable periodic walking at pre-determined fixed step lengths, while satisfying torque limits, ground reaction forces and other key constraints. Instead of pre-computing transition controllers between discrete elements of the gait library, at the beginning of a step, the distance to the next stepping stone is determined, and based on this, the gait library is linearly interpolated to provide a nominal controller with the desired step length in steady state. To ensure precise foot placement during transients associated with varying distances between stepping stones, the CBF-QP based controller relaxes the tracking behavior of the nominal gait and strictly enforces a set of state-dependent safety constraints that guide the swing foot trajectory to the discrete footholds. Our method enables dealing with a continuum of widely varying desired foothold separations, while achieving foot placement on small footholds. This work builds off our recent work on precise footstep placement using CBF with one nominal walking gait [17] and gait libraries in [6]. In this paper, we will use exponential control barrier function (ECBF) [18] to handle safety constraints. In comparison to our prior work, this paper makes the following additional contributions:

- We present gait optimization and a gait-library-interpolation approach for achieving a continuum of desired step lengths in steady state.
- We incorporate exponential control Barrier functions and control Lyapunov functions to achieve precise transient footstep placement with the gait library approach.
- We significantly enlarge the range of variation on step length that can be handled.
- We provide a way to handle sustained step length perturbations.
- Through our QP-based real-time controller, we address simultaneously footstep placement, foot scuffing avoidance, friction constraints and input saturation.

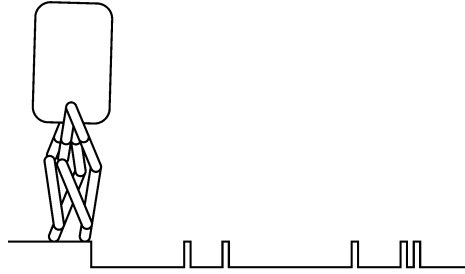


Fig. 1: The problem of dynamically walking over a randomly generated set of discrete footholds. Simulation video: https://youtu.be/udpxZUXBi_s.

The remainder of the paper is organized as follows. Section 2 presents the hybrid dynamical model of 2D MARLO, an underactuated planar bipedal robot. Section 3 presents gait optimization and a gait library interpolation strategy. Section 4 presents the proposed ECBF-CLF-QP based feedback controller for enforcing precise footstep placement for dynamic walking. Section 5 presents numerical validation of the controller on MARLO. Finally, Section 6 provides concluding remarks.

2 Dynamical Model for Walking

The bipedal robot shown in Fig. 2 is a planar representation of MARLO. Its total mass is 63 kg, with approximately 50% of the mass in the hips and 40% in the torso, and with light legs formed by a four-bar linkage. The robot is approximately left-right symmetric.

The configuration variables for the system can be defined as $q := (q_T, q_{1R}, q_{2R}, q_{1L}, q_{2L}) \in \mathbb{R}^5$. The variable q_T corresponds to the world frame pitch angle, while the variables $(q_{1R}, q_{2R}, q_{1L}, q_{2L})$ refer to the local coordinates for linkages. Each of the four linkages are actuated by a DC motor behind a 50:1 gear ratio harmonic drive, with the robot having one degree of underactuation. The four-bar linkage mechanism comprising of the leg coordinates (q_1, q_2) map to the leg angle and knee angle (q_{LA}, q_{KA}) , as $q_{LA} := \frac{1}{2}(q_1 + q_2)$ and $q_{KA} := q_2 - q_1$. With the state x denoting the generalized positions and velocities of the robot and u denoting the joint torques, a hybrid model of walking can be expressed as

$$\begin{cases} \dot{x} = f(x) + g(x)u & x \notin \mathcal{S} \\ x^+ = \Delta(x^-) & x \in \mathcal{S}, \end{cases} \quad (1)$$

where \mathcal{S} is the impact surface and Δ is the reset or impact map. A more complete description of the robot and a derivation of its model are given in [19].

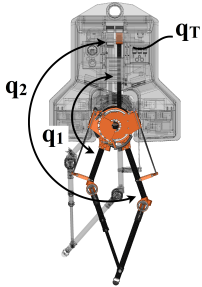


Fig. 2: Biped coordinates. The world frame pitch angle is denoted by q_T , while (q_1, q_2) are body coordinates. The model is assumed left-right symmetric.

3 Optimization and Gait library

Having described the dynamical model of MARLO, we will now present a model-based approach for designing a continuum of stable periodic walking gaits that satisfy physical constraints arising from the robot and its environment. The method combines virtual constraints, parameter optimization, and an interpolation strategy for creating a continuum of gaits from a finite library of gaits.

3.1 Gait Design Using Virtual Constraints

The nominal feedback controller is based on the virtual constraints framework presented in [21]. Virtual constraints are kinematic relations that synchronize the evolution of the robot's coordinates via continuous-time feedback control. One virtual constraint in the form of a parametrized spline can be imposed for each (independent) actuator. Parameter optimization is used to find the spline coefficients so as to create a periodic orbit satisfying a desired step length, while respecting physical constraints on torque, motor velocity, and friction cone. The optimization method used here is the direct collocation code from [12], although other methods, such as [11] or `fmincon` can be used as well.

The virtual constraints are expressed as an output vector

$$y = h_0(q) - h_d(s(q), \alpha), \tag{2}$$

to be asymptotically zeroed by a feedback controller. Here, $h_0(q)$ specifies the quantities to be controlled

$$h_0(q) = \begin{bmatrix} q_{LA}^{st} \\ q_{KA}^{st} \\ q_{LA}^{sw} \\ q_{KA}^{sw} \end{bmatrix}, \tag{3}$$

where st and sw designate the stance and swing legs, respectively, and $h_d(s, \alpha)$ is a 4-vector of Beziér polynomials in the parameters α specifying the desired

evolution of the $h_0(q)$, where s is a gait phasing variable defined as

$$s := \frac{\theta - \theta_{init}}{\theta_{final} - \theta_{init}}, \quad (4)$$

with $\theta = q_T + q_{LA}^{st}$ being the absolute stance leg angle.

The cost function and constraints for the optimization are formulated as in [21] [Chap. 6.6.2], with the constraints given in Table 1 and the cost taken as integral of squared torques over step length:

$$J = \frac{1}{L_{step}} \int_0^T \|u(t)\|_2^2 dt. \quad (5)$$

Table 1: Optimization constraints

Motor Torque	$ u \leq 5 \text{ Nm}$
Impact Impulse	$F_e \leq 15 \text{ Ns}$
Friction Cone	$\mu \leq 0.4$
Vertical Ground Reaction Force	$F_{st}^v \geq 200 \text{ N}$
Mid-step Swing Foot Clearance	$h_f _{s=0.5} \geq 0.1 \text{ m}$

Having presented an optimization approach to create an individual walking gait, we will next discuss the design of a finite set of gaits and a means to create from it a continuum of gaits, called the gait Library.

3.2 Gait Library and Interpolation

The optimization problem posed in the previous section is used to generate five gaits having step lengths $L_{step} = \{0.08, 0.24, 0.40, 0.56, 0.72\}$ meters¹. For values of step length between the discrete values, $L_{step,i}$, $1 \leq i \leq 5$, define the Beziér coefficients α in (2) by linear interpolation of the coefficients α_i for the five nominal step lengths. In particular, define,

$$\zeta(L_{step}) = \frac{L_{step} - L_{step,i}}{L_{step,i+1} - L_{step,i}}, \quad 1 \leq i \leq 4 \quad (6)$$

$$\alpha(L_{step}) = (1 - \zeta(L_{step}))\alpha_i + \zeta(L_{step})\alpha_{i+1}. \quad (7)$$

For step lengths longer than 0.72, linear extrapolation is used. As in [6, Eqn. (8,9)], this defines a continuum of gaits, called the gait library

$$\mathcal{A} = \{\alpha(L_{step}) \mid 0.08 \leq L_{step} \leq 0.72\}. \quad (8)$$

¹ The number of gaits is arbitrary. A finer grid did not change the results. A coarser grid was not tried.

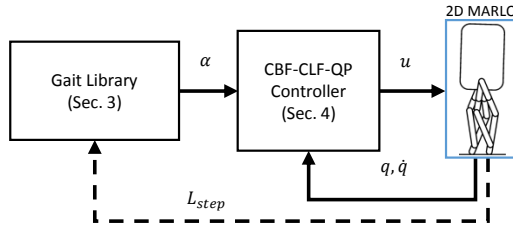


Fig. 3: Diagram of the controller structure integrating the gait library and CBF based controller. Solid lines represent signals in continuous time; dashed lines represent signals in discrete time.

The update resets the periodic orbit to adapt the step length, while respecting the physical constraints and approximately optimizing the cost on the periodic point. During a transient following a change in commanded step length, the footstep placement and optimization constraints shown in Table.1 are not guaranteed to be satisfied. In the next Section, we will introduce the method of control Barrier functions to handle real-time constraints on footstep placement, scuffing avoidance, friction cone, and input saturation.

4 Control Barrier Function based controller for stepping stones

Having presented the creation of a library of gaits for a small set of step lengths and an associated switching controller, we now discuss the low-level continuous-time controller design that uses control Lyapunov functions for driving the outputs in (2) to zero and control Barrier functions for strictly enforcing foot placement constraints. We will incorporate both features through a quadratic program that will also be used to enforce torque saturation input constraints and state constraints such as ground contact force and friction cone constraints. The control diagram for the combination of gait library and CBF based controller is shown in Fig.3.

4.1 Control Lyapunov Function based Quadratic Programs Revisited

In this section we will review recent innovations in control Lyapunov functions for hybrid systems and control Lyapunov function based quadratic programs, introduced in [3] and [10] respectively.

Input-output linearization Consider the control output vector $y(q)$ defined in (2) with vector relative degree 2, then the second derivative takes the form

$$\ddot{y} = L_f^2 y(q, \dot{q}) + L_g L_f y(q, \dot{q}) u. \quad (9)$$

We can then apply the following pre-control law

$$u(q, \dot{q}) = u^*(q, \dot{q}) + (L_g L_f y(q, \dot{q}))^{-1} \mu, \quad (10)$$

where

$$u^*(q, \dot{q}) := -(L_g L_f y(q, \dot{q}))^{-1} L_f^2 y(q, \dot{q}), \quad (11)$$

and μ is a stabilizing control to be chosen. Defining transverse variables $\eta = [y, \dot{y}]^T$, and using the IO linearization controller above with the pre-control law (10), we have,

$$\begin{bmatrix} \dot{\eta} \\ \ddot{\eta} \end{bmatrix} = \dot{\eta} = F\eta + G\mu \quad (12)$$

where

$$F = \begin{bmatrix} 0 & I \\ 0 & 0 \end{bmatrix}, \quad G = \begin{bmatrix} 0 \\ I \end{bmatrix}. \quad (13)$$

CLF-based Quadratic Programs A control approach based on control Lyapunov functions, introduced in [3], provides guarantees of exponential stability for the transverse variables η . In particular, a function $V(\eta)$ is a *exponentially stabilizing control Lyapunov function (ES-CLF)* for the system (12) if there exist positive constants $c_1, c_2, \lambda > 0$ such that

$$c_1 \|\eta\|^2 \leq V(\eta) \leq c_2 \|\eta\|^2, \quad (14)$$

$$\dot{V}(\eta, \mu) + \lambda V(\eta) \leq 0. \quad (15)$$

In our problem, we chose a CLF candidate as follows

$$V(\eta) = \eta^T P \eta, \quad (16)$$

where P is the solution of the Lyapunov equation $A^T P + P A = -Q$ (with A being a Hurwitz matrix such that $\dot{\eta} = A\eta$ is exponentially stable, and Q being any symmetric positive-definite matrix). The time derivative of the CLF (16) is computed as

$$\dot{V}(\eta, \mu) = L_{\bar{f}} V(\eta) + L_{\bar{g}} V(\eta) \mu, \quad (17)$$

where

$$L_{\bar{f}} V(\eta) = \eta^T (F^T P + P F) \eta; \quad L_{\bar{g}} V(\eta) = 2\eta^T P G. \quad (18)$$

The CLF condition in (15) then takes the form

$$L_{\bar{f}} V(\eta) + L_{\bar{g}} V(\eta) \mu + \lambda V(\eta) \leq 0. \quad (19)$$

If this inequality holds, then it implies that the output η will be exponentially driven to zero by the controller. The following CLF-QP based controller, initially presented in [10], takes the form:

CLF-QP:

$$\begin{aligned} \mu^* = \operatorname{argmin}_{\mu, d_1} \quad & \mu^T \mu + p_1 d_1^2 \\ \text{s.t.} \quad & \dot{V}(\eta, \mu) + \lambda V(\eta) \leq d_1 \quad \text{(CLF)} \\ & A_{AC}(q, \dot{q}) \mu \leq b_{AC}(q, \dot{q}) \quad \text{(Constraints)} \end{aligned} \quad (20)$$

where p_1 is a large positive number that represents the penalty of relaxing the CLF condition (15) and A_{AC} , b_{AC} represent additional constraints such as torque constraints, contact force constraints, friction constraints and joint limit constraints. This formulation opened a novel method to guarantee stability of the nonlinear systems with respect to additional constraints, such as torque saturation in [10] and L_1 adaptive control in [16].

Having presented control Lyapunov function based quadratic programs, we will next introduce control Barrier functions and control Barrier function based quadratic programs.

4.2 Control Barrier Function based Quadratic Programs

Exponential Control Barrier Function Consider an affine control system:

$$\dot{x} = f(x) + g(x)u \quad (21)$$

with the goal to design a controller to keep the state x in the set

$$\mathcal{C} = \{x \in \mathbb{R}^n : h(x) \geq 0\} \quad (22)$$

where $h : \mathbb{R}^n \rightarrow \mathbb{R}$ is a continuously differentiable function.

In order to systematically design safety-critical controllers for higher order relative degree constraints, we will use ‘‘Exponential Control Barrier Functions’’ (ECBFs), introduced in [18].

With application to precise footstep placement, our constraints will be position based, $h(q) \geq 0$, which has relative degree 2. For this problem, we can design an Exponential CBF as follows:

$$B(q, \dot{q}) = \dot{h}(q, \dot{q}) + \gamma_1 h(q), \quad (23)$$

and the Exponential CBF condition will be simply defined as:

$$\dot{B}(q, \dot{q}, u) + \gamma B(q, \dot{q}) \geq 0, \quad (24)$$

where $\gamma_1 > 0, \gamma > 0$. Enforcing (24) will then enforce $B(q, \dot{q}) \geq 0$. Moreover, we also note that by plugging the ECBF (23) into the condition (24), we have,

$$\left(\frac{d}{dt} + \gamma_1\right) \circ \left(\frac{d}{dt} + \gamma\right) \circ h(q) \geq 0. \quad (25)$$

Thus, γ_1, γ play the role of pole locations for the constraint dynamics $\ddot{h}(q, \dot{q}, u)$.

Combination of ECBF and CLF-QP We have the exponential CBF constraint $B(x)$ as a real-valued function with relative degree one, i.e.,

$$\dot{B}(x, u) = L_f B(x) + L_g B(x) u, \quad (26)$$

where $L_g B \neq 0$. Substituting for the pre-control law (10), we can rewrite the above in terms of the control input μ , i.e., $\dot{B}(x, \mu)$. We then have the following QP based controller:

ECBF-CLF-QP:

$$\begin{aligned} \mu^* = \underset{\mu, d_1}{\operatorname{argmin}} \quad & \mu^T \mu + p_1 d_1^2 \\ \text{s.t.} \quad & \dot{V}(\eta, \mu) + \lambda V(\eta) \leq d_1 && \text{(CLF)} \\ & \dot{B}(x, \mu) + \gamma B(x) \geq 0 && \text{(ECBF)} \\ & u_{min} \leq u(\mu) \leq u_{max} && \text{(Input Saturation)} \end{aligned} \quad (27)$$

where $B(x)$ is constructed based on the safety constraint $h(x)$ in (23).

Having revisited control Barrier function based quadratic programs, we will now formulate our controller to achieve dynamic walking with precise footstep placements.

4.3 Safety-Critical Control for Dynamical Bipedal Walking with Precise Footstep Placement

Constraints on Footstep Placement If we want to force the robot to step onto a specific position (see Fig. 1), we need to guarantee that the step length when the robot swing foot hits the ground is bounded within a given range $[l_{min}; l_{max}]$. Let $h_f(q)$ be the height of the swing foot to the ground and $l_f(q)$ be the distance between the stance and swing feet. We define the step length at impact as,

$$l_s := l_f(q)|_{h_f(q)=0, \dot{h}_f(q, \dot{q}) < 0}. \quad (28)$$

The discrete foothold constraint to be enforced then becomes,

$$l_{min} \leq l_s \leq l_{max}. \quad (29)$$

However, in order to guarantee this final impact-time constraint, we construct a state-based constraint for the evolution of the swing foot during the whole step, so that at impact the swing foot satisfies the discrete foothold constraint (29). We now offer a solution for this issue. The geometric explanation for this is presented in Fig. 4. If we can guarantee the trajectory of the swing foot, F , to be bounded between the domain of the two circles O_1 and O_2 , it will imply that the step length when the swing foot hits the ground is bounded within $[l_{min}; l_{max}]$. These two constraints can be represented as:

$$O_1 F \leq R_1 + l_{max}; \quad O_2 F \geq \sqrt{R_2^2 + \left(\frac{l_{min} + l_0}{2}\right)^2}.$$

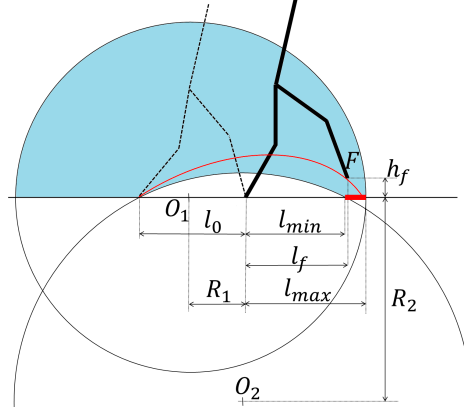


Fig. 4: Geometric explanation of CBF constraints for the problem of bipedal walking over discrete footholds. If we can guarantee the trajectory of the swing foot F (the red line) to be limited in the blue domain, we will force our robot to step onto a discrete foothold position (thick red range on the ground). This approach therefore also provides a safety guarantee against foot scuffing or swing foot being always above the ground prior to contact.

When the swing foot hits the ground at the end of the step, the step length is l_s (see (28)), implying the discrete foothold constraint (29).

Remark 1. (Avoiding Foot Scuffing) In this paper, we want to deal with a very large range of step lengths. Implementing the switching gait library based controller results in frequent foot scuffing for the swing foot since the gait library offers no guarantees on foot scuffing and other constraints during transient steps. We can address this issue by constructing a Barrier that enforces no foot scuffing. We do this by enlarging the circle O_2 , which guarantees the lower bound constraint on step length ($l_s \geq l_{min}$), to also ensure foot scuffing avoidance simultaneously. In particular, the circle O_2 intersects with the swing foot position at start of gait and therefore ensures no scuffing for the entire step, especially when combined with the gait library switching controller.

We now define the two barrier constraints based on this approach, through the position constraints

$$\begin{aligned} h_1(q) &= R_1 + l_{max} - O_1 F \geq 0, \\ h_2(q) &= O_2 F - \sqrt{R_2^2 + \left(\frac{l_{min} + l_0}{2}\right)^2} \geq 0. \end{aligned} \quad (30)$$

We can then apply the ECBF-CLF-QP based controller (27) for the above constraints. This involves creating two barriers B_1, B_2 for the corresponding position functions h_1, h_2 respectively.

Constraints on Friction Cone In bipedal robotic walking, contact force constraints are very important for the problem of robotic walking. Any violation of these constraints will result in the leg slipping and the robot potentially falling. Although walking gait optimization is usually designed to respect these constraints, however, we cannot guarantee these constraints when switching between different walking gaits. In particular, we consider, $F(x, u)$ and $N(x, u)$, the friction force and vertical contact force between the stance foot and the ground. Then, the constraints to avoid slipping during walking are,

$$\begin{aligned} N(x, u) &\geq \delta_N > 0, \\ \frac{|F(x, u)|}{|N(x, u)|} &\leq k_f. \end{aligned} \quad (31)$$

where δ_N is a positive threshold for the vertical contact force, and k_f is the friction coefficient. We enforce the above ground contact constraints with $\delta_N = 150(N)$, $k_f = 0.6$.

Remark 2. Note that since the gait optimization is performed offline, we enforce stricter constraints (ground reaction force $F_{st}^v \geq 200(N)$ and friction cone $\mu \leq 0.4$) (see Table 1), allowing for a margin of safety. These constraints hold only for the gaits in the gait library and not for the transient steps generated by the gait library controller. Our ECBF-CLF-QP controller enforces the constraints $F_{st}^v \geq 150(N)$ and friction cone $\mu \leq 0.6$ in real-time for the transient steps.

We then have the following ECBF-CLF-QP based controller that can handle simultaneously footstep placement, scuffing avoidance, friction constraint and input saturation:

$$\begin{aligned} \mu^* &= \underset{\mu, d_1}{\operatorname{argmin}} \quad \mu^T \mu + p_1 d_1^2 \\ \text{s.t.} \quad & \dot{V}(\eta, \mu) + \lambda V(\eta) \leq d_1 && \text{(CLF)} \\ & \dot{B}_1(x, \mu) + \gamma B_1(x) \geq 0 && \text{(ECBF on } l_s \leq l_{max}) \\ & \dot{B}_2(x, \mu) + \gamma B_2(x) \geq 0 && \text{(ECBF on } l_s \geq l_{min} \\ & && \text{\& Foot Scuffing)} \\ & N(x, u(\mu)) \geq \delta_N > 0 && \text{(Normal Force)} \\ & \frac{|F(x, u(\mu))|}{|N(x, u(\mu))|} \leq k_f && \text{(Friction Cone)} \\ & u_{min} \leq u(\mu) \leq u_{max} && \text{(Input Saturation)} \end{aligned} \quad (32)$$

Remark 3. Note that all the constraints are affine in μ and thus the above optimization problem is still a quadratic program that can be solved in real-time.

Remark 4. The gait library approach offers a switching strategy under a wide range of step lengths. Based on the desired step length, the interpolation between different gaits in the library will result in a new walking gait for the next step. If

the system state is on or close enough to the periodic orbit, it will converge to the desired step length while maintaining physical constraints mentioned in Table.1. However, in our problem, we want the robot to be able to switch between two gaits with very different step lengths, the initial condition is basically very far from the periodic orbit of the next step. Therefore, the transition to the new gait is not guaranteed to satisfy constraints such as friction constraints as well as scuffing avoidance. In the simulation, these two main reasons make the gait library approach fail almost all the time.

Note that the CBF-CLF-QP controller in [17] is only based on one nominal gait and tries to adjust the control inputs so as to enforce the footstep placement constraint, friction constraints and input saturation while following the nominal gait. Due to the limitation of having only one walking gait, the working range of step length is therefore limited.

In this paper, we attempt to combine the advantages of each method and develop the ECBF-CLF-QP controller with foot scuffing constraints and combine it with the gait library approach (see Fig.3). Given a desired step length, the gait library assigns an interpolated gait for the next walking step and the ECBF-CLF-QP controller tracks the outputs corresponding to this gait by solving a quadratic program in real-time to find the control input that follows this new gait while maintaining all above constraints (footstep placement, friction constraints, scuffing avoidance and input saturation).

In the next Section, we present numerical validation of our proposed controller on the dynamical model of the bipedal robot MARLO.

5 Numerical Validation

In this Section, we will demonstrate the effectiveness of the proposed method by conducting numerical simulations on the model of MARLO. We validate the performance of our proposed approach through dynamic bipedal walking on MARLO, while simultaneously enforcing foot placement, scuffing avoidance, ground contact force constraints and input saturation. Furthermore, in order to demonstrate the effectiveness of the method, we compare three controllers on different ranges of desired step lengths:

$$\left\{ \begin{array}{l} \text{I: Gait Library} \\ \text{II: CBF (with nominal step length of 56 cm)} \\ \text{III: CBF \& Gait Library} \end{array} \right. \quad (33)$$

For each range of step length (see Table 2), we randomly generated 100 problem sets, where each set has 10 randomly placed “stepping stones” with a stone size of 5 (cm) (see Fig. 1). The controller is successful for a trial run if the bipedal robot is able to walk over this terrain without violation of foot placement or friction constraints. The percentage of successful tests for each of the three controllers is tabulated in Table 2 for various ranges of step lengths.

Table 2: **(Main Result)** Percentage of successful tests of three controllers (see (33)) with different ranges of desired step length.

Step Length Range (cm)	Gait Library	CBF	Gait Library & CBF
[50:60]	6%	100%	100%
[40:70]	1%	44%	100%
[30:80]	1%	17%	100%
[25:85]	1%	12%	100%
[20:90]	1%	3%	97%
[15:95]	1%	0%	92%
[10:100]	0%	0%	78%

The approach based on the combination of CBF and Gait Library outperforms the approaches that rely on only the CBF or only the Gait Library. For example, with the step length range of [20:90] (cm), the percentage of successful tests on controller III (CBF and Gait Library) is 97 %, while that of controller II (CBF only) and controller I (Gait Library only) are just 3% and 1% respectively. Thus the proposed controller not only achieves dynamic walking over discrete footholds, it also dramatically increases the range of step lengths that are handled compared to our prior work in [17].

We show here one simulation of MARLO walking over 20 stepping stones with desired step lengths randomly generated in the range of [10 : 100] (cm), where the stone size is smaller, i.e., $l_{max} - l_{min} = 2$ (cm). Fig. 5 shows the satisfaction of foot step placement constraints as well as CBF constraints, without a violation of the friction cone or input saturation (see Figs. 6 and 7).

In order to illustrate how aggressively our proposed method can traverse a set of stepping stones, Fig. 8 shows a simulation where the robot has to switch between very a large step length (95 cm) and a very small step length (15 cm).

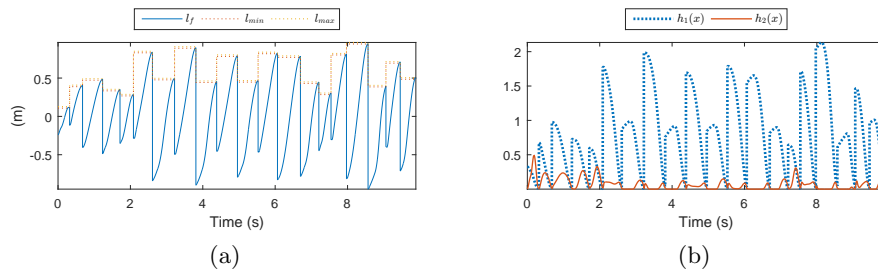


Fig. 5: (a) Footstep placement constraint: $l_{min} \leq l_s \leq l_{max}$, where the step length l_s is the value of the distance between swing and stance feet l_f at impact (see (28)). (b) CBF constraints: $h_1(x) \geq 0, h_2(x) \geq 0$ (see (30)).

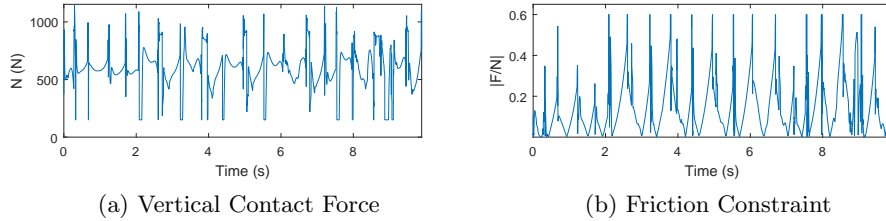


Fig. 6: Friction constraints: $N \geq 150(N)$ and $|F/N| \leq 0.6$.

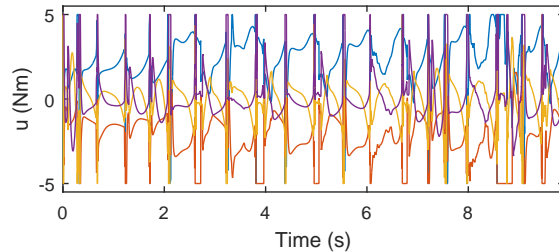


Fig. 7: Control inputs are saturated at 5 (Nm) ($|u| \leq 5$); recall the 50:1 gear ratio from the motors to the links.

6 Conclusion

We have presented a model-based control framework that allows transition among widely and randomly varying stepping stones, without an exponential explosion in the number of pre-computed motion primitives. The control design begins with model-based optimization producing a small number of periodic walking gaits that meet desired physical constraints and span a range of step lengths. In an outer-loop, a gait library is formed by interpolating this set of walking gaits to provide controllers that realize a continuum of step lengths. In an inner-loop, a quadratic program mediates safety, interpreted as landing the swing foot on a stepping stone, and performance, which involves joint-level tracking commands, friction cone, scuffing avoidance and torque bounds. The resulting controller achieved dynamic walking while enforcing strict constraints on foot step placement at impact, resulting in dynamic walking over stepping stones. Numerical illustration of the proposed method on MARLO, an underactuated bipedal robot, included the robot handling random step length variations that are between $[10 : 100]$ (cm) with a foot placement precision of 2 (cm).

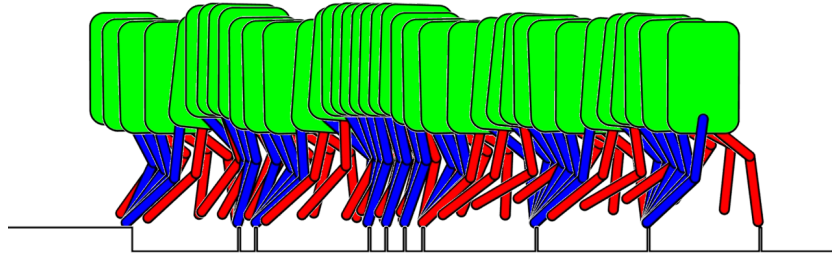


Fig. 8: Simulation of MARLO walking over stepping stones with desired step lengths of [95 15 95 15 15 15 95 95 95 15 15 15](cm) and stone size of 2 (cm). For clarity of visualization, the rear links of the 4-bar are suppressed. Simulation video: <https://youtu.be/udpxZUXBi.s>.

In future work, the method will be extended to 3D robots so that the stepping-stone course in the W-Prize [1] can be attempted. In addition to the challenges of 3D locomotion, the heights of the stepping stones vary over the course. Even more interesting, the stones are specified to be constructed from standardized blocks that may topple over.

References

1. “The W-Prize on stepping stones,” <http://www.wprize.org/SteppingStones.html>.
2. A. D. Ames, J. Grizzle, and P. Tabuada, “Control barrier function based quadratic programs with application to adaptive cruise control,” in *IEEE Conference on Decision and Control*, 2014, pp. 6271–6278.
3. A. D. Ames, K. Galloway, J. W. Grizzle, and K. Sreenath, “Rapidly Exponentially Stabilizing Control Lyapunov Functions and Hybrid Zero Dynamics,” *IEEE Trans. Automatic Control*, vol. 59, no. 4, pp. 876–891, 2014.
4. J. Chestnutt, J. Kuffner, K. Nishiwaki, and S. Kagami, “Planning biped navigation strategies in complex environments,” in *IEEE International Conference on Humanoid Robotics*, 2003, pp. 117–123.
5. J. Chestnutt, M. Lau, G. Cheung, J. Kuffner, J. Hodgins, and T. Kanade, “Footstep planning for the honda asimo humanoid,” *Proceedings of the 2005 IEEE International Conference on Robotics and Automation.*, pp. 629 – 634, 2005.
6. X. Da, O. Harib, R. Hartley, B. Griffin, and J. Grizzle, “From 2d design of under-actuated bipedal gaits to 3d implementation: Walking with speed tracking,” *IEEE Access*, vol. PP, no. 99, pp. 1–1, 2016.
7. R. Deits and R. Tedrake, “Footstep planning on uneven terrain with mixed-integer convex optimization.” *Proceedings of the 2014 IEEE/RAS International Conference on Humanoid Robots*, pp. 279–286, 2014.
8. R. L. H. Deits, “Convex segmentation and mixed-integer footstep planning for a walking robot,” Master’s thesis, Massachusetts Institute of Technology, 2014.
9. R. Desai and H. Geyer, “Robust swing leg placement under large disturbances,” *Proceedings of the IEEE International Conference on Robotics and Biomimetics (ROBIO)*, pp. 265–270, 2012.

10. K. Galloway, K. Sreenath, A. D. Ames, and J. W. Grizzle, "Torque saturation in bipedal robotic walking through control lyapunov function based quadratic programs," *IEEE Access*, vol. PP, no. 99, p. 1, April 2015.
11. A. Hereid, C. M. Hubicki, E. A. Cousineau, J. W. Hurst, and A. D. Ames, "Hybrid zero dynamics based multiple shooting optimization with applications to robotic walking," in *2015 IEEE International Conference on Robotics and Automation (ICRA)*. IEEE, 2015, pp. 5734–5740.
12. M. S. Jones, "Optimal control of an underactuated bipedal robot," Master's thesis, Oregon State University, ScholarsArchive@OSU, 2014.
13. S. Kajita, F. Kanehiro, K. Kaneko, K. Fujiwara, K. Harada, K. Yokoi, and H. Hirukawa, "Biped walking pattern generation by using preview control of zero-moment point," *Proceedings of the IEEE International Conference on Robotics and Automation (ICRA)*, vol. 2, pp. 1620 – 1626, 2003.
14. J. J. Kuffner, K. Nishiwaki, S. Kagami, M. Inaba, and H. Inoue, "Footstep planning among obstacles for biped robots," *Proceedings of the 2001 IEEE/RSJ International Conference on Intelligent Robots and Systems*, vol. 1, pp. 500 – 505, 2001.
15. P. Michel, J. Chestnutt, J. Kuffner, and T. Kanade, "Vision-guided humanoid footstep planning for dynamic environments," in *Humanoids*, 2005, pp. 13–18.
16. Q. Nguyen and K. Sreenath, "L1 adaptive control for bipedal robots with control lyapunov function based quadratic programs," in *American Control Conference*, 2015, pp. 862–867.
17. —, "Safety-critical control for dynamical bipedal walking with precise footstep placement," in *The IFAC Conference on Analysis and Design of Hybrid Systems*, 2015, pp. 147–154.
18. —, "Exponential control barrier functions for enforcing high relative-degree safety-critical constraints," in *American Control Conference*, 2016, pp. 322–328.
19. A. Ramezani, J. W. Hurst, K. Akbari Hamed, and J. W. Grizzle, "Performance Analysis and Feedback Control of ATRIAS, A Three-Dimensional Bipedal Robot," *Journal of Dynamic Systems, Measurement, and Control*, vol. 136, no. 2, 2014.
20. M. Rutschmann, B. Satzinger, M. Byl, and K. Byl, "Nonlinear model predictive control for rough-terrain robot hopping," *Proceedings of the IEEE/RSJ International Conference on Intelligent Robots and Systems (IROS)*, pp. 1859–1864, 2012.
21. E. R. Westervelt, J. W. Grizzle, C. Chevallereau, J. Choi, and B. Morris, *Feedback Control of Dynamic Bipedal Robot Locomotion*, ser. Control and Automation. Boca Raton, FL: CRC, June 2007.
22. T. Yang, E. Westervelt, A. Serrani, and J. P. Schmiedeler, "A framework for the control of stable aperiodic walking in underactuated planar bipeds," *Autonomous Robots*, vol. 27, no. 3, pp. 277–290, 2009.